Proceedings of the 2013 IEEE International Conference on
Cyber Technology in Automation, Control and Intelligent Systems
May 26-29, 2013, Nanjing, China

Inverse Kinematics and Workspace Analysis of a Bio-inspired Flexible Parallel Robot

Bingtuan Gao*, Honggang Song†, Lixia Sun†, Yi Tang*
*School of Electrical Engineering, Southeast University, Nanjing, China
Email: gaobingtuan@seu.edu.cn
†College of Energy and Electrical Engineering, Hohai University, Nanjing,China

***Abstract*—This paper presents the inverse kinematics and workspace analysis of a cable-driven flexible parallel robot mimicking pitch and roll movements of human neck. The fixed base and moving platform of the robot are connected by three cables and a compression spring. The spring serves as cervical spine to support and facilitate the motion of moving platform corresponding to human head. The cables serve as the muscles around human neck to drive the robot. Quaternion method is employed to obtain the rotation transformation matrix between the base coordinate frame attached to the fixed base and the moving coordinate frame attached to the moving platform. By combining the equations of force and moment balance together with lateral bending equations of the compression spring, inverse kinematics of the parallel robot is solved. Based on the force and moment balance model, the wrench closure workspace of the robot is analyzed with constrain of positive cable tension. Simulations were performed to demonstrate the correctness and feasibility of the inverse kinematics and workspace analysis of the parallel robot.**

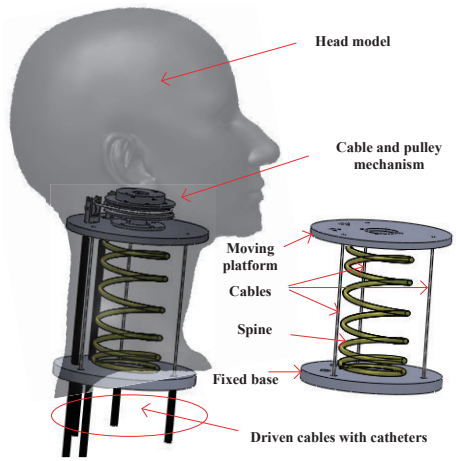

Fig. 1. Overview of the robotic neck mechanism design

I. INTRODUCTION

In harmful environments existing nuclear radiation or chemical substance, people need to wear personal protective equipments such as donning respirators or chemical-resistant jackets. These personal protective equipments will generate acoustic noises when users moves especially their heads. These noises may obscure people's hearing of useful information and make them perform wrong actions, resulting in catastrophic consequences. Therefore, it is critical to analyze the effect of such noise on a human's hearing. To conduct such an acoustic investigation, a presented method is to use a robot head for such experiments instead of relying on humans to perform head movements which may costs higher and not achieve the ideal outcome [1]. Based on the humanoid neck systems proposed in [1], [2], [3], this paper focuses on a simplified humanoid neck parallel robot where the compression spring serves as cervical spine and the three cables serve as the muscles around human neck, as shown in Fig. 1.

Compared to traditional robots, cable-driven parallel robots are relatively simple in form and possess some valuable characteristics such as large workspace, low inertia, high payload to weight ratio, transportability, reconfigurability, and fully remote actuation [4], [5]. The advantages make the cable-driven parallel robots a promising alternative to the rigid-link mechanisms in many industrial applications, such as load lifting and positioning [6] and wind tunnels [7].

The cable-driven parallel robot shown in Fig.1 belongs to the category of Incompletely Restrained Positioning Mechanisms (IRPM) according to Verhoeven [8]. In order to make all cables taut, the spring as the spine element is adopted which provided external load. This idea is not new. The head mechanism of SAYA is made up of a coil spring to support the head and several pneumatic artificial muscles placed around the spring to actuate the head [9]. For the iCub robot, aside from the serial neck design, two parallel mechanisms are implemented for the neck. The first one is based on a compression spring with three actuated cables separated 120° apart; the second one uses a 3 Degrees of Freedom (DOF) parallel mechanism with a central passive spherical strut [10]. The James humanoid robot also has a head similar to the first parallel mechanism of iCub [11]. However, they failed to make quantitative analysis on inverse kinematics of the robotic heads in the above papers.

In [3], we have proposed a 4 cables driven flexible humanoid neck system and analyzed the inverse kinematics and statics in detail. However, there is a redundancy to realize the Pitch and Roll of the moving platform driven by 4 cables which increases the cost of the system. Theoretically, realizing 2DOF of humanoid neck only need three 120° cables. Moreover, the workspace of the cable-driven parallel robot needed to be discussed. Since 3 cables driven parallel mechanism is the basis of studying multi-cables driven humanoid neck paral-

978-1-4799-0612-3/13/$31.00 © 2013 IEEE

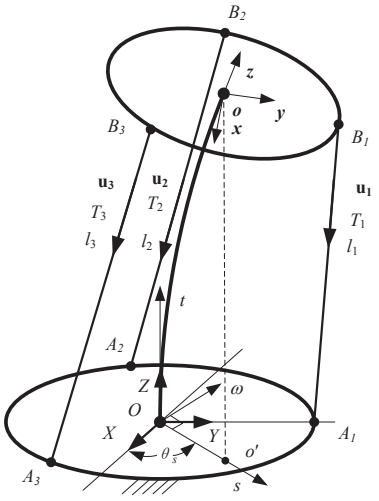

Fig. 2. Schematic of cable-driven and flexible parallel mechanism

lel mechanism, its inverse kinematics and statics is studied extensively in this paper. Consequently, based on the force and moment balance model, the Wrench Closure Workspace (WCW) of the robot is analyzed with constrain of positive cable tension.

The remaining sections of this paper are organized as follows: in Section II, descriptions of the mechanism including the notations used in this paper and the DOF parametrization for the mechanism are presented. After that, the inverse position and statics are solved simultaneously in Section III. Based on the statics, the WCW of the robot is analyzed in Section IV. Finally, conclusions are given in Section V.

II. CONFIGURATION OF THE MECHANISM

The structure of the proposed cable-driven parallel robot, as shown in Fig. 2 consists of four main components: fixed base, movable platform, three flexible cables with negligible mass and diameter, compression spine. The movable platform is driven by three cables and the connection points are $B_i (i = 1, 2, 3)$. The other end of each cable connects to the roller driven by a motor and the cables pass through the fixed base in the points A_i. A base coordinate frame $OXYZ$ is attached to the fixed base, with the origin of the frame is at the bottom center of the spring. A moving coordinate frame $oxyz$ is attached to the moving platform, with its origin at the top center of the spring. $\overrightarrow{OA_i}$ and $\overrightarrow{oB_i}$ are along the same direction in the initial configuration and both A_i and B_i are equidistance to each other on the circle with radii $|OA_i| = a$ and $|oB_i| = b$ with respect to the center O and o, respectively. Denote the force value along the cable as T_i , the cable length between A_i and B_i as l_i, and the unit vector for the direction of force in each cable as ${}^O\mathbf{u}_i$. In the plane O, o and o', a planar body frame Ost is attached to the spring. The origin is the same as the base coordinate frame $OXYZ$, the t-axis is the same as the Z-axis in frame $OXYZ$ and the s-axis is along $\overrightarrow{Oo'}$.

We assume the spring will bend in a plane. Moreover, since the torsional strength for spring compression is quite large, we also assume the moving platform does not rotate about the z-axis of the body frame $oxyz$. In this case, we need four parameters to define the configuration of the moving platform [3]:

- θ_s: angle between axis s and axis X (bending direction);
- θ_p: angle between the fixed base plane and the moving platform plane (bending amplitude);
- t_0: t coordinate for point o in the spring attached frame Ost (vertical length of the bending spring);
- s_0: s coordinate for point o in frame Ost (lateral translation for the bending spring).

There are only three independent parameters among them. Without loss of generality, we can consider s_0 to be the dependent parameter. In other words, once θ_s, θ_p and t_0 are given, s_0 can be solved. In this case, s_0 is considered as a parasitic motion that can be determined by the other three parameters. This parasitic motion is frequently encountered in parallel manipulators [12]. As defined by the IFToMM, the DOF is the number of independent coordinates needed to define the configuration of a mechanism [13]. According to this definition, this mechanism has only 3 DOF. θ_s and θ_p can describe the posture of the moving platform. We can get the poseture matrix when θ_s and θ_p have been given.

Assume e_1, e_2, e_3, and i_1, i_2, i_3 are sets of base in the base coordinate frame and the moving coordinate frame, respectively, $\mathbf{r} = r_1 i_1 + r_2 i_2 + r_3 i_3$ is a constant vector in the moving coordinate frame, and $\mathbf{q} = q_0 + q_1 i + q_2 j + q_3 k$ is a normalized quaternion. Then, $\mathbf{r}$ changes into $\mathbf{r}'$ whose component in the original coordinate frame is $\mathbf{r}' = r'_1 i_1 + r'_2 i_2 + r'_3 i_3$ when the moving coordinate frame turn into the base coordinate frame. Based on the theorem on quaternion[13], the relationship between r'_1, r'_2, r'_3 and r_1, r_2, r_3 is formulated as [14]:

$$\begin{aligned}[r'_1, r'_2, r'_3] &= [r_1, r_2, r_3] \cdot \begin{bmatrix} r_{11} & r_{12} & r_{13} \\ r_{21} & r_{22} & r_{23} \\ r_{31} & r_{32} & r_{33} \end{bmatrix} \\ &= [r_1, r_2, r_3] \cdot {}^O\mathbf{R}_o \end{aligned} \quad (1)$$

where

$$\begin{aligned} &r_{11} = q_0^2 + q_1^2 - q_2^2 - q_3^2, r_{12} = 2(q_1 q_2 + q_0 q_3), \\ &r_{13} = 2(q_1 q_3 - q_0 q_2); r_{21} = 2(q_1 q_2 - q_0 q_3), \\ &r_{22} = q_0^2 - q_1^2 + q_2^2 - q_3^2, r_{23} = 2(q_2 q_3 + q_0 q_1); \\ &r_{31} = 2(q_1 q_3 + q_0 q_2), r_{32} = 2(q_2 q_3 - q_0 q_1), \\ &r_{33} = q_0^2 - q_1^2 - q_2^2 + q_3^2. \end{aligned}$$

The components of $\mathbf{r}$ in the base coordinate frame are the same as the components of $\mathbf{r}'$ in the moving frame because $\mathbf{r}$ is a constant vector, namely:

$$\mathbf{r}' = [r'_1, r'_2, r'_3] \begin{bmatrix} i_1 \\ i_2 \\ i_3 \end{bmatrix} = [r_1, r_2, r_3] \begin{bmatrix} e_1 \\ e_2 \\ e_3 \end{bmatrix} \quad (2)$$

Combining (1) (2), we have:

$$\begin{bmatrix} e_1 \\ e_2 \\ e_3 \end{bmatrix} = {}^{O}\mathbf{R}_o \begin{bmatrix} i_1 \\ i_2 \\ i_3 \end{bmatrix}$$

One can see that ${}^{O}\mathbf{R}_o$ presents the relationship between the unit vectors of the two coordinate frames. i.e. ${}^{O}\mathbf{R}_o$ is the transformation matrix between the two coordinate frames. It also can be considered as the rotation about an axis $\boldsymbol{\omega}$ perpendicular to Os with an angle θ_p, where $\boldsymbol{\omega} = \begin{bmatrix} \omega_1 & \omega_2 & \omega_3 \end{bmatrix}^{\mathrm{T}} = \begin{bmatrix} -\sin\theta_s & \cos\theta_s & 0 \end{bmatrix}^{\mathrm{T}}$.

Consider that normalized quaternion $\mathbf{q} = q_0 + q_1 i + q_2 j + q_3 k$ can be also written as follows [14]:

$$\mathbf{q} = \cos\frac{\alpha}{2} + \boldsymbol{\omega}\sin\frac{\alpha}{2}$$

namely:

$$\cos\frac{\alpha}{2} + \boldsymbol{\omega}\sin\frac{\alpha}{2} = q_0 + q_1 i + q_2 j + q_3 k$$

where $\alpha = \theta_p$. We have:

$$\begin{aligned} &q_0 = \cos\tfrac{\alpha}{2}, q_1 = \omega_1 \sin\tfrac{\alpha}{2} = -\sin\theta_s \sin\tfrac{\theta_p}{2}, \\ &q_2 = \omega_2 \sin\tfrac{\alpha}{2} = \cos\theta_s \sin\tfrac{\theta_p}{2}, q_3 = \omega_3 \sin\tfrac{\alpha}{2} = 0 \end{aligned}$$

Substituting q_0, q_1, q_2, q_3 into ${}^{O}\mathbf{R}_o$, it can be rewritten as follows:

$${}^{O}\mathbf{R'}_o = \begin{bmatrix} t_{11} & t_{12} & t_{13} \\ t_{21} & t_{22} & t_{23} \\ t_{31} & t_{32} & t_{33} \end{bmatrix}$$

where

$$\begin{aligned} t_{11} &= \sin^2\theta_{\mathrm{s}} + \cos\theta_{\mathrm{p}}\cos^2\theta_{\mathrm{s}}, \\ t_{12} &= t_{21} = (\cos\theta_{\mathrm{p}} - 1)\cos\theta_{\mathrm{s}}\sin\theta_{\mathrm{s}} \\ t_{13} &= -t_{31} = \sin\theta_{\mathrm{p}}\cos\theta_{\mathrm{s}}, \\ t_{23} &= -t_{32} = \sin\theta_{\mathrm{p}}\sin\theta_{\mathrm{s}} \\ t_{22} &= \cos^2\theta_{\mathrm{s}} + \cos\theta_{\mathrm{p}}\sin^2\theta_{\mathrm{s}} \\ t_{33} &= \cos\theta_{\mathrm{p}} \end{aligned}$$

Consequently, the homogeneous transformation matrix between the moving frame and the base coordinate frame can be achieved as:

$${}^{O}\mathbf{T}_o = \begin{bmatrix} {}^{O}\mathbf{R'}_o & {}^{O}\mathbf{P}_o \\ 0 & 1 \end{bmatrix}$$

where ${}^{O}\mathbf{P}_o$ is the position vector of point o with respect to the base coordinate frame, and ${}^{O}\mathbf{P}_o = \begin{bmatrix} s_0\cos\theta_s & s_0\sin\theta_s & t_0 \end{bmatrix}^{\mathrm{T}}$.

III. INVERSE KINEMATIC AND STATICS ANALYSIS

The inverse position kinematics problem is stated as: given the desired DOF value $\mathbf{x} = \begin{bmatrix} \theta_s & \theta_p & t_0 \end{bmatrix}^{\mathrm{T}}$ to calculate the cable lengths l_i. The solution is straightforward calculating $l_i = \left\| {}^{O}T_o\overrightarrow{oB_i} - \overrightarrow{OA_i} \right\|$ if s_0 is solved from $\mathbf{x}$. However, s_0 cannot be arbitrarily assigned. This parasitic motion is a characteristic of the spring lateral bending, which is caused by the forces acting on the spring. These forces mainly are resulted from the pulling forces in the four cables and the mass of the payload. Therefore, we should combine the inverse position and statics in order to obtain a solution. The general procedure is [3]:

1) Transform all the cable forces to the equivalent force and moment applied at the springs top center.
2) Use the equivalent force and moment to get the desired spring lateral bending equations.
3) Solve s_0.
4) Solve the inverse position and statics.

A. Force and Moment Balance Equations

In order to sustain any external wrench $(\mathbf{F}, \mathbf{M})$ applied on the moving platform, all cables must be able to create tension forces to achieve equilibrium of the moving platform. Assume all the cable forces can be transformed into bending plane Ost, we can convert all the forces to two perpendicular forces F_1 and F_2 in the plane, and a moment $\mathbf{M}$ perpendicular to the plane at the spring's top center as shown in Fig. 3. The mass of the moving platform is taken as a mass point at the spring's top center with quantity m. The equilibrium conditions for force and moment at the moving platform are as follows:

$$\sum_{i=1}^{3} \mathbf{T}_i + \mathbf{F} = \mathbf{0} \tag{3}$$

$$\sum_{i=1}^{3} {}^{O}\mathbf{r}_i \times \mathbf{T}_i + \mathbf{M} = \mathbf{0} \tag{4}$$

where $\mathbf{T}_i = T_i {}^{O}\mathbf{u}_i = -T_i \frac{\mathbf{l}_i}{l_i}$ and ${}^{O}\mathbf{r}_i = {}^{O}\mathbf{R'}_o \cdot \overrightarrow{oB_i}$. Moreover, $\mathbf{F} = \begin{bmatrix} -F_1\sin\theta_s & -F_1\cos\theta_s & F_2 - mg \end{bmatrix}^{\mathrm{T}}$, $\mathbf{M} = \begin{bmatrix} M\sin\theta_s & -M\cos\theta_s & 0 \end{bmatrix}^{\mathrm{T}}$

Equations (3) and (4) can be decomposed into six equations. In the six equations, there are in total seven unknowns: T_1 to T_3 , F_1 , F_2 , M and s_0. Eliminating T_1 to T_3, an equation with only F_1, F_2, M and s_0 as the unknowns can be obtained:

$$\begin{aligned} & 2b\sin\theta_{\mathrm{s}}\sin\theta_{\mathrm{p}}{F_2}'s_0^2 \\ + \; & 2b(\sin\theta_{\mathrm{s}}\sin\theta_{\mathrm{p}}t_0F_1 + \sin\theta_{\mathrm{s}}\cos\theta_{\mathrm{p}}t_0{F_2}' \\ & + \sin\theta_{\mathrm{s}}\sin\theta_{\mathrm{p}}M + \frac{1}{2}a\sin\theta_{\mathrm{p}}\cos 2\theta_{\mathrm{s}}{F_2}')s_0 \\ + \; & b(2t_0^2\sin\theta_{\mathrm{s}}\cos\theta_{\mathrm{p}} - ab\sin\theta_{\mathrm{s}}\sin^2\theta_{\mathrm{p}} \\ & + a\sin\theta_{\mathrm{p}}\cos 2\theta_{\mathrm{s}}t_0)F_1 \\ - \; & ab\sin\theta_{\mathrm{p}}\sin\theta_{\mathrm{s}}\left(a - b\cos\theta_{\mathrm{p}}\right){F_2}' \\ - \; & 2t_0\sin\theta_{\mathrm{s}}\left(a - b\cos\theta_{\mathrm{p}}\right)M = 0 \end{aligned} \tag{5}$$

where ${F_2}' = F_2 - mg$.

Based on the lateral bending analysis of the compression spring as in [3], F_1 and M can be expressed as:

$$F_1 = D_1 s_0 + E_1 \tag{6}$$

$$M = D_2 s_0 + E_2 \tag{7}$$

where

$$\begin{aligned} D_1 &= -\frac{a_2c_1 - a_1c_2}{a_2b_1 - a_1b_2}, E_1 = -\frac{a_2d_1 - a_1d_2}{a_2b_1 - a_1b_2}, \\ D_1 &= -\frac{b_2c_1 - b_1c_2}{a_1b_2 - a_2b_1}, E_2 = -\frac{b_2d_1 - b_1d_2}{a_1b_2 - a_2b_1}, \end{aligned}$$

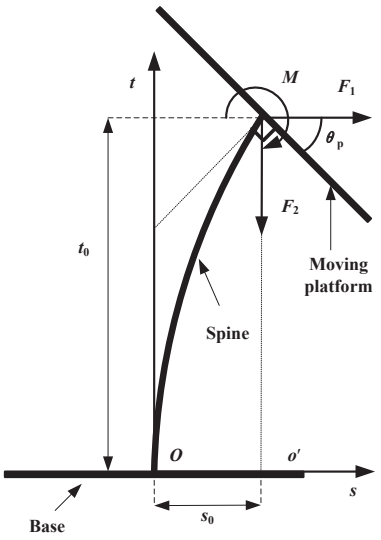

Fig. 3. Force and moment balance system

$$
\begin{aligned}
a_1 &= 1-\cos\left(\sqrt{F_2/\beta}t_0\right),\\
b_1 &= \sqrt{\beta/F_2}\sin\left(\sqrt{F_2/\beta}t_0\right)-t_0\cos\left(\sqrt{F_2/\beta}t_0\right),\\
c_1 &= -F_2\cos\left(\sqrt{F_2/\beta}t_0\right),\\
d_1 &= 0;\\
a_2 &= \sqrt{F_2/\beta}\sin\left(\sqrt{F_2/\beta}t_0\right),\\
b_2 &= \cos\left(\sqrt{F_2/\beta}t_0\right)+t_0\sqrt{F_2/\beta}\sin\left(\sqrt{F_2/\beta}t_0\right)-1,\\
c_2 &= F_2\sqrt{F_2/\beta}\sin\left(\sqrt{F_2/\beta}t_0\right),\\
d_2 &= -F_2\tan\theta_{\mathrm{p}}.
\end{aligned}
$$

Substituting (6) and (7) into (5), the following equation is obtained:

$$As_0^2+Bs_0+C=0 \tag{8}$$

where

$$
\begin{aligned}
A &= 2b\sin\theta_{\mathrm{p}}\sin\theta_{\mathrm{s}}\left({F_2}'+t_0D_1+D_2\right)\\
B &= (2bt_0^2\cos\theta_{\mathrm{p}}\sin\theta_{\mathrm{s}}-ab^2\sin^2\theta_{\mathrm{p}}\sin\theta_{\mathrm{s}}\\
&\quad +abt_0\sin\theta_{\mathrm{p}}\cos2\theta_{\mathrm{s}})D_1\\
&\quad -2t_0\sin\theta_{\mathrm{s}}\left(a-b\cos\theta_{\mathrm{p}}\right)D_2\\
&\quad +2bt_0\sin\theta_{\mathrm{s}}\left({F_2}'\cos\theta_{\mathrm{p}}+E_1\sin\theta_{\mathrm{p}}\right)\\
&\quad +2b\sin\theta_{\mathrm{p}}\left(E_2\sin\theta_{\mathrm{s}}+\frac{1}{2}a{F'}_2\cos2\theta_{\mathrm{s}}\right)\\
C &= (2bt_0^2\cos\theta_{\mathrm{p}}\sin\theta_{\mathrm{s}}-ab^2\sin^2\theta_{\mathrm{p}}\sin\theta_{\mathrm{s}}\\
&\quad +abt_0\sin\theta_{\mathrm{p}}\cos2\theta_{\mathrm{s}})E_1\\
&\quad -ab\sin\theta_{\mathrm{p}}\sin\theta_{\mathrm{s}}\left(a-b\cos\theta_{\mathrm{p}}\right){F_2}'\\
&\quad -2t_0\sin\theta_{\mathrm{s}}\left(a-b\cos\theta_{\mathrm{p}}\right)E_2
\end{aligned}
$$

Equation (8) is a Quadratic equation and A, B, C are known when θ_{p} and θ_{s} are given. Then, s_0 can be obtained by solving the (8). Once s_0 is obtained, all the other unknowns can be calculated.

B. Numerical Implementations

The inverse position and statics analysis were implemented in MATLAB. Parameters of spring compression for the prototype are shown in TABLE I, where l_0 is the initial length, h_0 is the pitch, G is the shearing modulus, E is the elastic modulus, r is the radius, d is the diameter of the spring wire and K is the spring constant. Therefore the moment of inertia I of the cross-section of the spring wire and the flexural rigidity β_0 are obtained by the following equations:

$$I=\frac{\pi d^4}{64}=9.811\times10^{-12}\mathrm{m}^4,\beta_0=\frac{2EGIh_0}{\pi r\left(E+2G\right)}=0.2321$$

TABLE I
PARAMETERS OF SELECTED COMPRESSED COIL SPRING

l_0(m)	h_0(m)	G(Gpa)	E(Gpa)	r(m)	d(m)	K(N/m)
0.1016	0.0195	81.2	196.5	0.02273	0.00376	4153

The other parameters are chosen as a = b = 0.05 m and m = 0.05 kg. The implementation is performed with a fixed t_0 = 0.085 m because in real applications t_0 can only be used to adjust the pretension force in the three cables. By varying θ_p from 0 to π/8 and θ_s from 0 to 2π, we can obtain the results shown in Fig. 4, where the cables lengths and forces are shown as the z coordinate.

We can have three observations from Fig. 4. First of all, the length and force complement each other for each cable. In other words, when the length is small, the force will be large. This is in accordance with our intuition because when the cable length is small, the cable should exert a large force on the moving platform.The second observation from Fig. 4 is that when θ_p is large, the variations of both the force and length are also large. This is because the more we want to bend the moving platform, the larger force we need to act on it. Finally, for a fixed θ_p, the length and force curves for all the cables with θ_s from 0 to 2π are symmetric. This cannot be seen clearly from Fig. 4; therefore, we plot all the cable lengths and forces with θ_p = π/8 and t_0 = 0.085 m in Fig. 5 (a) and (b), respectively. It is clear that all the curves have the same profile, but with different phases.

IV. WORKSPACE ANALYSIS

For a cable-driven parallel robot, its workspace is the space where sets of positive cable tensions exist because they are needed to constrain the moving platform all the time regardless of any external wrench [15]. The workspace of the robot in this paper is defined as the set of the center points of moving platform while all the cables are in tension. Assume the result wrench of the cables applied on the moving platform as $\boldsymbol{\eta}$, then $\boldsymbol{\eta}=-\left[\begin{array}{cc}\mathbf{F} & \mathbf{M}\end{array}\right]^{\mathrm{T}}$, and (3), (4) can be rewritten as:

$$\left\{\begin{array}{ccc}{}^{O}\mathbf{u}_1 & {}^{O}\mathbf{u}_2 & {}^{O}\mathbf{u}_3\\ {}^{O}\mathbf{r}_1\times{}^{O}\mathbf{u}_1 & {}^{O}\mathbf{r}_2\times{}^{O}\mathbf{u}_2 & {}^{O}\mathbf{r}_3\times{}^{O}\mathbf{u}_3\end{array}\right\}\left\{\begin{array}{c}T_1\\T_2\\T_3\end{array}\right\}=\boldsymbol{\eta} \tag{9}$$

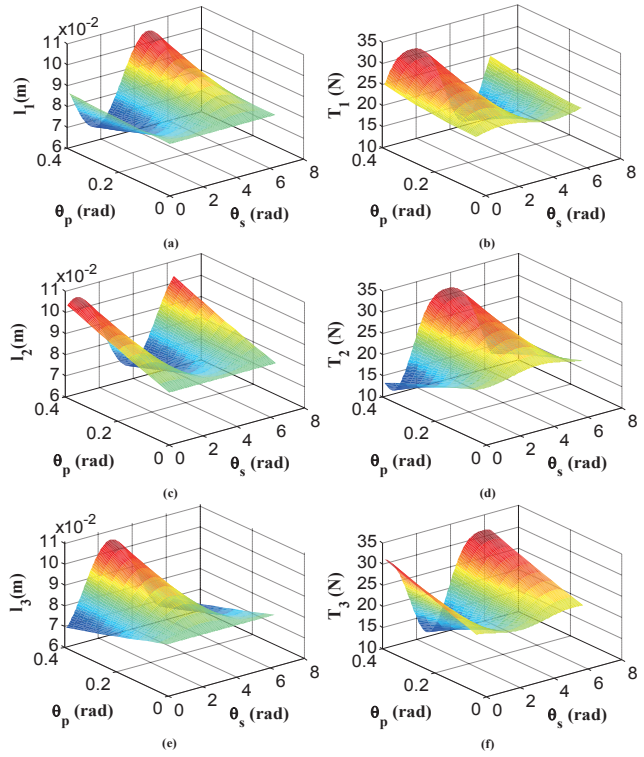

Fig. 4. Inverse position and statics illustration

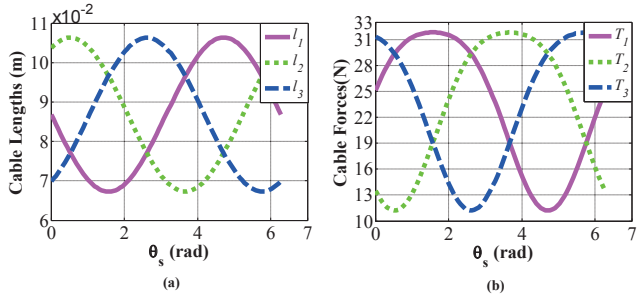

Fig. 5. Inverse position and statics with θ_p=π/8 and t_0=0.085m

Assume $\xi_i = \begin{bmatrix} {}^{O}\mathbf{u}_i & {}^{O}\mathbf{r}_i \times {}^{O}\mathbf{u}_i \end{bmatrix}^{\mathrm{T}}$ is defined as the line vector of the ith cable. The following equation is obtained:

$$A\mathbf{t} = \boldsymbol{\eta} \tag{10}$$

where $A = \begin{Bmatrix} \boldsymbol{\xi}_1 & \boldsymbol{\xi}_2 & \boldsymbol{\xi}_3 \end{Bmatrix}$ and $\mathbf{t} = \begin{Bmatrix} T_1 & T_2 & T_3 \end{Bmatrix}^{\mathrm{T}}$. A is called Structure Matrix of the cable-driven robot, which is highly relied on the configuration of the robot and gesture of the moving platform, and A is fundamental to all the analysis of the cable-driven parallel robot. $\mathbf{t}$ is the tension vector of the 3 cables. Equation (10) is the static equilibrium model of the 3DOF cable-driven parallel robots driven by 3 cables.

If the moving platform is included within the WCW, the following condition have to be satisfied:

$$A\mathbf{t} = \boldsymbol{\eta}, \forall \boldsymbol{\eta}, \mathbf{t} > 0 \tag{11}$$

When external wrench $\boldsymbol{\eta}$ applied on the moving platform, the general solution of the force on the cables can be described as:

$$\mathbf{t} = \mathbf{t}_p + \mathbf{t}_h \tag{12}$$

where $\mathbf{t}_p$ is the particular solution of (11), and $\mathbf{t}_h$ is homogenous solution of (11).

Verhoeven [16] points out that the sufficient and necessary condition of the moving platform inclusion within the WCW is:

$$\begin{cases} rank(A) = 3 \\ Null(A) \cap R_+^3 \neq \emptyset \end{cases} \tag{13}$$

where $Null(A)$ is the null space of structure matrix A, R_+^3 is the positive set of 3 dimension real space, and $\emptyset$ is the empty set.

As shown in (13), if structure matrix A is full rank, i.e. $rank(A) = 3$, the cable-driven parallel robot can realize 3DOF motion. Otherwise, when $rank(A) < 3$, the line vectors ξ_i become linear dependant, therefore, the wrenches on the cable cannot span the 3-dimension space, and there are wrench deficiency in the robot. The cable-driven robot cannot realize the 3DOF motion. Therefore, the structure matrix A should be full rank to avoid singularity and the rank of A can be easily obtained by software MATLAB command rank().

The second condition of (13) can be interpreted as:

$$A\mathbf{t} = 0, \mathbf{t}_i > 0 \tag{14}$$

The solution of (14) is the homogenous solution $\mathbf{t}_h$. The method to compute the second condition is shown below. $\mathbf{t}_h$can also be described as[14]:

$$\mathbf{t}_h = \zeta_1\boldsymbol{\varepsilon}_1 + \zeta_2\boldsymbol{\varepsilon}_2 + \cdots + \zeta_k\boldsymbol{\varepsilon}_k, \tag{15}$$

where $k = m-n$, m is the number of cables and n is the DOF of the cable-driven parallel robot. $\boldsymbol{\varepsilon}_j$(j=1,2,...,k) is basis of the null space of structure matrix A and can be easily obtained when the structure matrix A is known. ζ_j an arbitrary real constant. The equivalent form of the second condition in (13) is:

$$\zeta_1\boldsymbol{\varepsilon}_1 + \zeta_2\boldsymbol{\varepsilon}_2 + \cdots + \zeta_k\boldsymbol{\varepsilon}_k > 0 \tag{16}$$

Equation (16) can be altered to m inequalities with the unknown parameters, if there were solutions of (16), the second condition of (13) would be realized. For the robot proposed in this paper, $m = n = 3$, equation (11) has a unique solution $\mathbf{t}_p$. Therefore, it is not necessary to judge (16). Then, the method which identifies whether the pose belonging to the translational WCW consists of the following four steps:

1) Fix the orientation of the moving platform, i.e. the Euler angel of the moving platform.
2) At a prescribed space discrete the space by the certain step into discrete points. The structure matrix A is computed at each point by the method mentioned in (10).
3) To justified whether the structure matrix A is full rank or not. If so, the point is inclusion within the WCW, go to next step.
4) Recording all the discrete points meeting the step 3), and the space composed by these points is the translational WCW.

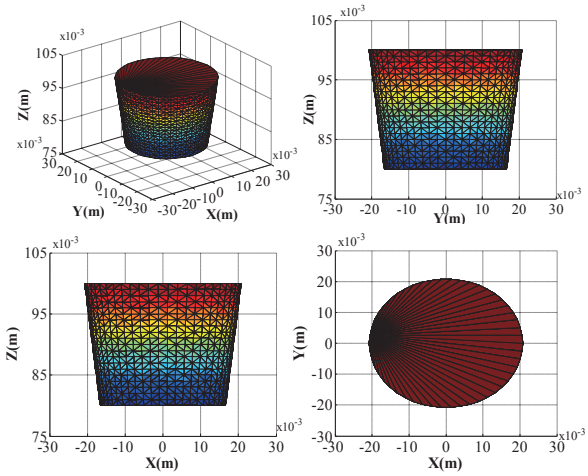

Fig. 6. The translational WCW of the cable-driven parallel robot when angle θ_p=π/8, a=b=0.05m

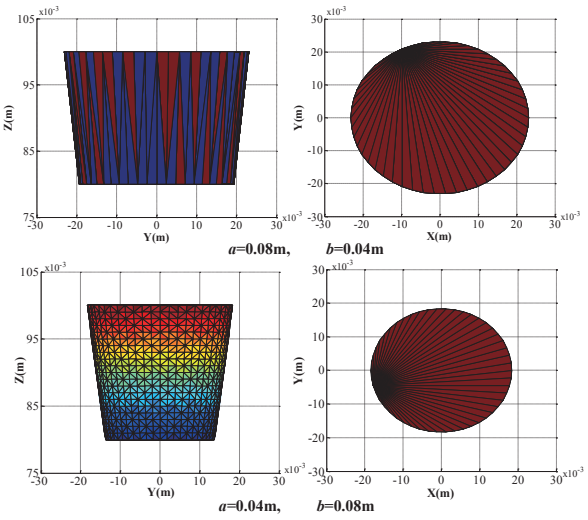

Fig. 7. The variation of workspace with different a and b

For illustration of the workspace analysis of the robot presented in this paper, the numerical solutions are calculated to show the characteristic of the robot. According to the method mentioned above, fix the angle θ_p=π/8, and discrete the rectangle space $(x \in [-0.03, 0.03], y \in [-0.03, 0.03], z \in [0.08, 0.1])$ at certain step. Based on the above four steps , the Cartesian 3D space and 2D space are drawn in Fig. 6. As shown in Fig. 6, one can see that the translational WCW is a inverted cone. In fact, the translational WCW is various with different values of a/b. Generally, the volume of the translational WCW of the robot will increase with the increase of value of a/b. The workspace of the robot with a=0.08m, b=0.04m and a=0.04m, b=0.08m is shown in Fig. 7. It is shown that the volume of the workspace with $a/b = 2$ is larger than one with $a/b = 0.5$.

V. CONCLUSIONS

This paper provide a bio-inspired flexible parallel robot whose moving platform and the base are connected with flexible supportive compression spring spine and 3 driving cables. Inverse kinematics and WCW of the robot are analyzed and numerical implemented. It is shown that inverse position of the robot can be solved by combined the force and torque balance equations together with the lateral bending equations of the spring spine. Numerical implementations shows that the translational WCW is a inverted cone and generally the volume of the translational WCW of the robot will increase as the increase of value a/b (connecting radii of the driving cables w. r. t. the base to the moving platform).

ACKNOWLEDGEMENT

The work is partially supported by National Science Foundation of China with No. 11102039 and the Opening Fund of Jiangsu Key Laboratory of Remote Measurement and Control Technology with No. 7722009001.

REFERENCES

[1] B. Gao, J. Xu, J. Zhao, et al, "A Humanoid Neck System Featuring Low Motion-Noise," Journal of Intelligent and Robotic Systems, vol.67, pp.101-116, 2012.

[2] B. Gao, N. Xi, Y. Shen, J. Zhao and R. Yang, "Development of a low motion-noise humanoid neck: Statics analysis and experimental validation," in: Proc. IEEE Int. Conf. on Robotics and Automation, Anchorage, AK, pp. 1203-1208, 2010.

[3] B. Gao, J. Xu, J. Zhao, N. Xi, "Combined Inverse Kinematic and Static Analysis and Optimal Design of a Cable-Driven Mechanism with a Spring Spine," Advanced Robotics, Vol. 26, pp. 8-9, 2012.

[4] S. Behzadipour, A. Khajepour, "Cable-based robot manipulators with translational degrees of freedom," in: Industrial Robotics: Theory, Modeling and Control, S. Cubero Ed. Austrial: ARS, pp. 211-236, 2006.

[5] X. Diao and O. Ma, "Force-closure analysis of 6-DOF cable manipulators with seven or more cables," Robotica, vol.27, pp.209-215, 2009.

[6] J. Albus, R. Bostelman, N. Dagalakis, "The nist robocrane," Journal of Robotic Systems ,vol.10, pp.709-724, 1993.

[7] P. Lafourcade, M. Llibre, "Design of a parallel wire-driven manipulator for wind tunnels," in: Pro. of the Workshop on Fundamental Issues and Future Research Directions for Parallel Mechanisms and Manipuloators. Quebec, Canada,pp.187-194, 2002.

[8] R. Verhoeven, M. Hiller, S. Tadokoro, "Workspace, stiffness, singularities and classification of tendon-driven Stewart platforms," in: Pro. of Int. Symposium on Advances in Robot Kinematics, pp.105-114, 1998.

[9] T. Hashimoto, S. Hitramatsu, T. Tsuji and H. Kobayashi, "Development of the face robot SAYA for rich facial expressions," in: Proc. SICECICASE Int. Joint Conf., Busan, pp. 5423-5428, 2006.

[10] R. Beira, M. Lopes, M. Praca, *et. al*, "Design of the robot-Cub (iCub) head," in: Proc. IEEE Int. Conf. on Robotics and Automation, Orlando, FL, pp. 94-100, 2006.

[11] F. Nori, L. Jamone, G. Metta, and G. Sandini, "Accurate control of a human-like tendon-driven neck," in: IEEE International Conference on Humanoid Robots, Pittsburgh, Pennsylvania, USA, pp. 371-378, 2007.

[12] J. A. Carretero, R. P. Podhorodeski, M. A. Nahon, and C. M. Gosselin, "Kinematic analysis and optimization of a new three degree-offreedom spatial parallel manipulator," ASME J. Mech. Des., vol. 122, pp. 17-24, 2000.

[13] G. Gogu, "Mobility of mechanisms: a critical review," Mech. Mach. Theory, vol.40, pp.1068-1097, 2005.

[14] G. Cheng, *The quaternion method and applications*, Hunan, China: NUDT Publish House, 1991.

[15] Y. Zhang, X. Dai, Yi, Yang, "Workspace analysis of a novel 6-dof cable-driven parallel robot," in: IEEE International Conference on Robotics and Biomimetic, pp.2403-2408, 2009

[16] R. Verhoeven, "Analysis of the Workspace of Tendon-based Stewart Platforms," Ph.D. dissertation, German. Duisburg: Duisburg-Essen University, 2004.